Journal of Applied Polymer Science

Highly crystalline and oriented high-strength poly(ethylene terephthalate) fibers by using low molecular weight polymer

Huseyin Avci,[1,2] Mesbah Najafi,[1] Ali Kilic,[3] Richard Kotek[1]

[1]College of Textiles, Textile Engineering Chemistry and Science, North Carolina State University, Raleigh, North Carolina
[2]Metallurgical and Materials Engineering, Eskisehir Osmangazi University, Eskisehir, Turkey
[3]Department of Textile Engineering, Istanbul Technical University, Istanbul, Turkey
Correspondence to: R. Kotek (E-mail: rkotek@ncsu.edu)

ABSTRACT: High-strength poly(ethylene terephthalate) (PET) fibers were obtained using low molecular weight (LMW) polymervia horizontal isothermal bath (hIB), followed by postdrawing process. We investigated the unique formations of different precursors, which differentiated in its molecular orientation and crystalline structures from traditional high-speed spinning PET fibers. Sharp increase in crystallinity was observed after drawing process even though the fibers showed almost no any crystallinity before the drawing. Properties of as-spun and drawn hIB and control filaments at different process conditions were compared. As would be expected, performances of resulted treated undrawn and drawn fibers have dramatically improved with developing unique morphologies. Tenacities more than 8 g/d for as-spun and 10 g/d for drawn treated fibers after just drawn at 1.279 draw ratio were observed. These performances are considerably higher than that of control fibers. An explanation of structural development of high-strength fibers using LMW polymer spun with hIB is proposed. © 2015 Wiley Periodicals, Inc. J. Appl. Polym. Sci. **2015**, *132*, 42747.

KEYWORDS: extrusion; fibers; mechanical properties; polyesters; X-ray

Received 25 March 2015; accepted 18 July 2015
DOI: 10.1002/app.42747

INTRODUCTION

High-strength polyester fibers are widely used in industry and our daily lives. Hence, studies on structural improvement of filament and its relation to production conditions have been examined carefully by researchers for many years. This resulted in 60% of the world's total polyester production having been consumed as fiber in 2010.[1] In general, zone drawing/zone annealing, microwave heating, one or two step drawing high-speed spinning, vibrational hot drawing, two-step spin draw processes, solution spinning, and solid-state extrusion are the most important production methods to manufacture high-performance polyester fibers.[2,3] Structural development of fibers in one-step high-speed spinning process is limited even if it appears promising in the case of economical and high throughputs. Therefore, two-step spin-draw and multistep drawing processes are widely accepted and utilized to obtain high modulus and tenacity polyester filaments.[2,4] On the other hand, the solution spinning technique is one of the crucial methods by using ultra-high molecular weight polymers to produce high-performance poly(ethylene terephthalate) (PET) fibers, but use some organic solvents raise questions about their toxicity.[5,6] This method is expensive and the production speed is slow. Sometimes more than one bath is required in the production lines and a very high draw ratio (DR) is needed to manufacture high-performance fibers.

Full understanding of precursors for crystallization and crystallization in polyester fibers is limited because of fast crystallization kinetic and the different formation of precursors. According to process conditions and polymer properties, a number of precursor models have been proposed. These precursors can be nematic, smectic, other less unidentified structures, and sometimes microvoids and/or banded structure can be associated with these forms.[7] In addition, all these forms have some common structural properties, as they are highly oriented but have noncrystallized molecular chains or chain segments. Nicholson *et al.*[8] have observed mesophase formation by drawing at the drawing temperature of 110°C with the DR of 4 using a very low oriented as-spun yarn. After the drawing process, the fibers were rapidly cooled to inhibit the crystallization, which showed a different usual form of triclinic and were described as "mesophase" form. However, this mesophase form, yet still exhibiting spatial order, was not very stable, and the annealing process could easily destroy it. In addition, Carr *et al.*[9] have produced nematic phase by drawing PEN: Polyethylene naphthalate films uniaxially at 120°C at the DRs range from 3.5 to 5.5 with observing long-range noncrystalline order when the

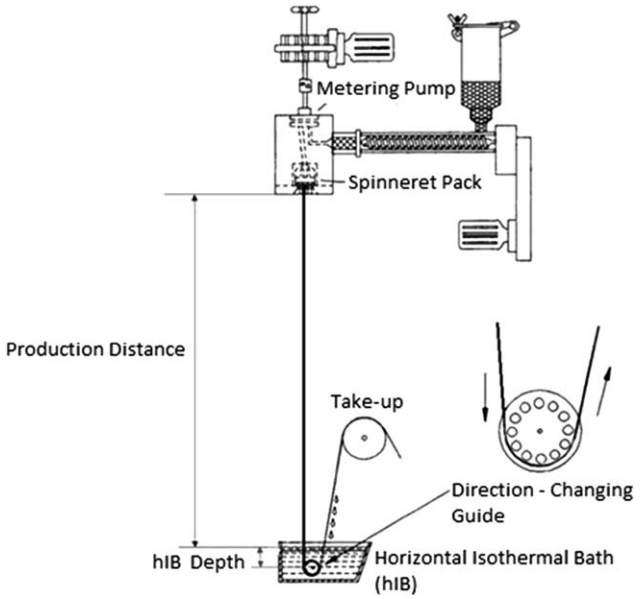

Figure 1. Melt spinning process with hIB spinning system.[18]

drawing temperature increased to 140°C for the films which showed a partially crystalline morphology. Generally, the mesophase forms when the sample is cooled rapidly after the processing to inhibit any crystallization. Afterwards, the drawing process can be applied at the temperature close to the glass transition temperature (T_g) or between glass transition and crystal melting temperature.[10] The critical DR is also very important because it sets up the onset of the crystallization. As seen in the past, the effect of temperature and DRs is significant for crystallization in the polymers. Higher DRs for PET increase the rate of strain-induced crystallization; however, the higher temperature will lead to an increase in molecular mobility to promote relaxation and crystallization.

Commonly, strain-induced crystallization occurs for PET materials, which are mechanically drawn close to the T_g within the temperature range between 20°C and 80.[11] Alfonso *et al.*[12] studied the crystallization kinetics in the orientated state for PET filaments. They showed that the orientation of the amorphous phase is very important and has a very strong relationship with crystallization and the rate of crystallization. In addition, increasing the temperature to a certain point causes an increase in the crystallinity.

On the other hand, Smith and Steward[13] investigated the rate of crystallization by carefully drawing different oriented noncrystalline PET fibers at 100°C, 120°C, and 150°C. Afterwards, the produced fibers were quenched rapidly to prevent any crystalline formation. It has been demonstrated that the degree of orientation had a great influence on the rate of crystallization. The resulting fibers showed the nucleation and initial growth of crystallites as a very rapid process for oriented PET at 120°C, which is about the order of milliseconds. However, when unoriented fibers were used, the crystallization time was several minutes. Moreover, Lu and Hay[14] observed that the crystallization rate for a strain-induced mechanism was much higher than a thermally induced mechanism at the same temperature. It was explained that the entropy of extension is the main factor, which increases the driving force for crystallization while reducing the free energies for nucleation and crystal growth. It has been also observed[14] the lower degree of orientation and crystallinity after increasing the temperature at a certain point of strain rate and elongation because of increasing molecular chain relaxation.

As a result, many researchers have investigated many structural developments to understand and make a better correlation between internal structure and material performance. Consequently, the researchers have developed numerous production techniques to improve the material's mechanical and thermal properties. One of the most important methods was revealed in the 1990s, a novel melt-spinning process with the liquid isothermal bath (LIB).[6,7,15–17] In this method, the resulted as-spun fibers had a very high degree of orientation and low and/or no crystallinity but had a high tenacity and modulus. Superior fiber mechanical properties were observed by drawing the fibers spun with LIB to a low DR. The synthetic melt spun fibers were extruded into a LIB, which should be at least 30°C above the T_g of the polymer with the take-up speed between 3000 and 7000 m/min. Numerous attempts have been performed by varying the liquid's temperature, liquid depth, distance between the spinneret and the tank, take-up speed, etc., to observe and make correlation between the resulted fibers' performance and process conditions. These studies have concluded that the high level of threadline stress, which occurred during the fibers moving through the liquid, hindered the molecular chains and segments mobility to form a very high orientation level and effectively prevent the crystal growth for undrawn filaments. This method was eventually modified by the utilization of a horizontal liquid isothermal bath (hIB),[7] to reduce energy consumption. It requires less capital equipment and can be used in large-scale production setting. As a result, hIB technique is simpler, safer, and can be applied to many different types of thermoplastic polymers.

Almost all researchers have been using high molecular weight polymers for their studies to produce high-performance fibers, also for the hIB method as well. For this study, we will present, for the first time, the spinning of high-strength PET fibers by using a low molecular weight polymer via hIB method with unusual structural developments.

EXPERIMENTAL

Materials and Production Methodology

Fiber forming PET chips having intrinsic viscosity (IV) of 0.65 dL/g was used in this study. The PET chips were vacuum dried at 140°C for 16 h. As-spun PET fibers with and without hIB were produced by using a Fourne single-screw extruder, which had a single hole with a hyperbolic spinneret with 0.6 mm exit diameter with the take-up speeds around 3000 m/min. Figure 1 shows that the production parameters which we used during the fiber production.

Modified Instron tensile testing equipment with a 60 cm long heating tube was used to draw fibers with the draw speed of 50 mm/min, and the draw temperature of 220°C.

Experiments and Characterization

Vibromat ME Tester equipment was used to determine denier of the monofilaments. The measurements are based on the resonance frequency principle. The fiber modulus and tenacity (gf/denier), in addition to the percentage strain at break, were observed via a MTS Q-test/5 universal testing machine using TestWorks 4EM V4.11B software according to ASTM (American Society for Testing and Materials) D3822.

Fiber surface and cross-section morphology were investigated using JEOL 6400 model of a cold field emission scanning electron microscope after fiber coating with a layer of Au/Pd at 0.5–30 keV accelerating voltage. The fiber cross-section was obtained to put the fibers into the liquid nitrogen and then broken apart in it.

X-ray generator that is Rigaku SmartLab X-ray diffractometer (XRD) equipped with CuK_{α} radiation source, $\lambda = 1.542$ Å, was operated at the power of 40 kV and 44 mA. The diffracting intensities were determined every 0.02° from 2θ scans in the range of 5–40°. Crystallites sizes were determined by using the Scherrer equation:[19]

$$L_{hkl} = \frac{K\lambda}{\beta \cos \Theta} \quad (1)$$

where β is the peak half width, K is taken to be unity, λ is the radiation wavelength (1.542 Å), and θ is the Bragg angle.

DSC (Differential Scanning Calorimetry) measurements were performed on a Perkin Elmer Diamond DSC Model 7 with Pyris software version 5. A small amount of 3–5 mg of the fibers was used for the DSC measurements with the heating rate of 20°C/min under a flow of nitrogen gas up to 280°C. Degree of crystallinity of PET fibers was calculated[20] from eq. (2):

$$\text{Degree of crystallinity } (\%) = \frac{\Delta H_f \times 100}{\Delta H_f^0} \quad (2)$$

where ΔH_f is the heat of fusion of PET fibers. ΔH_f^0 is the heat of fusion of 100% crystalline PET which is 140 J/g.[21]

Density measurements for all untreated and treated fibers were carried out by using ASTM D1505-10 standard. The experiment was run at 23°C by using a density gradient column containing sodium bromide solution (NaBr) in the density range of 1.335–1.415 g/cm^3. The volume fraction crystallinity (X_v) was determined from eq. (3):[22]

$$X_v = \frac{p - p_a}{p_c - p_a} \quad (3)$$

where p is the determined fiber density, p_a and p_c are the density of the amorphous and crystalline phases with the values of 1.335 and 1.455 g/cm^3, respectively.

Birefringence for the fibers was observed by using a Nikon polarizing microscope. At least three individual sample measurements were done for each fiber sample. A series of mineral oil refractive index liquids were used as an immersion liquid. The mean birefringence values were determined with the eq. (4):[15]

$$\Delta n = n_{II} - n_{\perp} \quad (4)$$

where n_{II} and $n_{\perp}$ are parallel and perpendicular refractive index of the sample, respectively.

RESULTS AND DISCUSSION

Mechanical Properties of the PET Fibers Spun With and Without hIB

In general, polymer chips having a high intrinsic viscosity (IV) close to 1 are used to produce high-tenacity PET fibers by achieving a high degree of the orientation for the undrawn fibers and the formation of tie chains connecting to the crystals. Hence, high tenacity and modulus fiber products can be obtained. However, it is known that the threadline dynamics of the fibers can be controlled with a liquid isothermal bath (hIB) spinning followed by a hot drawing process to improve the morphology of the fibers. Therefore, different set of as-spun fibers with a lower IV of 0.65 dL/g PET chips were spun with the hIB technology at take-up speed in the range of 2900–3000 m/min. Fiber properties of the as-spun and control fibers of each process were compared. Unlike PET control samples, the hIB as-spun and drawn fibers showed unique structural developments with demonstration of high tenacity and high modulus. The spinning conditions and comparison of the mechanical fiber properties of the hIB as-spun, control fibers, and the fibers after hot drawing process are listed in Tables (I–III), respectively.

As can be seen from Table II, the results indicated that the fibers' tenacity significantly increased with hIB technology. PET fibers tenacity increased by ca. 58%, 95%, 88%, and 90% from 4.19 ± 0.10 g/d to 6.60 ± 0.26, 8.19 ± 0.09, 7.87 ± 0.12, and 7.97 ± 0.13 g/d for undrawn fibers at 90 cm distance between the spinneret and tank with the bath temperature of 60°C, 100°C, 125°C, and 140°C, respectively. At the same time, the modulus tremendously increased by ca. 70%, 80%, 58%, and 86% from 64.62 ± 3.83 g/d to 109.54 ± 6.39, 116.52 ± 9.19, 102.40 ± 4.93, and 120.14 ± 4.05 g/d at the same production parameters. In addition, the percentage of elongation decreased from 73.50 ± 6.74 to 33.38 ± 4.23, 24.55 ± 2.79, 28.57 ± 2.57, and 25.50 ± 1.35% for the undrawn hIB fibers with the bath temperature of 60, 100, 125, and 140°C by ca. 55%, 67%, 61%, and 65% respectively.

It is obvious that the hIB fibers have not only a higher initial modulus and higher strength, but also a lower percent elongation at break than those of the control fibers. In the study, the effect of changes in the mechanical properties of PET fibers was assessed in terms of its tenacity, modulus, and elongation at break for different distances between the spinneret and hIB bath. The highest tenacity and modulus of 8.04 ± 0.14 g/d (1.02 GPa) and 120.52 ± 4.33 g/d (15.32 GPa) by the increasing ca. 270.51% and 215.25% from the control sample without hIB, respectively, were obtained by using the hIB technology at the bath temperature of 140°C with 120 cm distance (see Tables I and II) for the undrawn fibers. This performance for the treated as-spun fibers is very surprising and tremendous because the

Table I. Spinning Conditions of PET Fibers Spun With and Without hIB

Sample ID	Take-up speed (m/min)	Liquid temp. (°C)	Liquid depth (cm)	Distance (cm)	Denier
PET0	2910			90	9.20 ± 0.25
PET00	2910	CONTROL FIBERS		120	10.93 ± 0.39
PET000	2910			150	10.14 ± 0.18
PET1	2880			90	10.86 ± 0.15
PET11	2885	60	20	120	10.30 ± 0.15
PET111	2900			150	11.12 ± 0.22
PET2	2913			90	10.29 ± 0.08
PET22	2913	100	20	120	10.98 ± 0.18
PET222	2913			150	12.13 ± 0.36
PET3	2923			90	10.44 ± 0.10
PET33	2931	125	20	120	10.61 ± 0.32
PET333	2919			150	11.02 ± 0.40
PET4	2921			90	10.35 ± 0.07
PET44	2909	140	20	120	10.08 ± 0.21
PET444	2909			150	9.77 ± 0.13

traditional PET fibers can show this performance after very high DRs and more than two step drawing processes by using high molecular weight polymers. In the case of 150 cm production distance, the significant effect of the hIB spinning system on fiber tenacity and modulus was observed. As shown in Table II, a positive improvement is found between the hIB bath temperature and the tenacity values of PET fibers spun with hIB at 150 cm production distance between the spin pack and the tank.

Table II. Mechanical Properties of PET AsSpun Fibers Spun With and Without hIB

Sample ID	Tenacity (g/d)	Modulus (g/d)	Elongation (%)
PET0	4.19 ± 0.10	64.62 ± 3.83	73.50 ± 6.74
PET00	2.17 ± 0.08	38.23 ± 3.20	137.47 ± 10.29
PET000	2.05 ± 0.04	27.22 ± 5.80	160.14 ± 26.84
PET1	6.60 ± 0.26	109.54 ± 6.39	33.38 ± 4.23
PET11	6.26 ± 0.31	105.72 ± 5.69	39.21 ± 5.87
PET111	6.05 ± 0.24	103.33 ± 5.35	51.45 ± 5.17
PET2	8.19± 0.09	116.52 ± 9.19	24.55 ± 2.79
PET22	7.85 ± 0.14	116.94 ± 6.55	22.13 ± 2.88
PET222	7.41 ± 0.21	103.59 ± 6.06	24.97 ± 4.44
PET3	7.87 ± 0.12	102.40 ± 4.93	28.57 ± 2.57
PET33	7.91 ± 0.13	108.36 ± 5.04	27.14 ± 2.68
PET333	7.66 ± 0.19	103.53 ± 5.21	24.49 ± 4.57
PET4	7.97 ± 0.13	120.14 ± 4.05	25.50 ± 1.35
PET44	8.04 ± 0.14	120.52 ± 4.33	28.14 ± 3.68
PET444	8.07 ± 0.12	118.05 ± 6.50	26.00 ± 2.51

Associated with this matter, an interesting point of data shows which of the modulus values for the bath temperature of 60°C, 100°C, and 125°C of the as-spun fibers are very close to each other at about 103 g/d. The modulus value has reached approximately 118 g/d for the undrawn fibers spun with hIB when the liquid temperature was set to 140°C. The tenacity value increased from 2.05 ± 0.04 g/d to 8.07 ± 0.12 g/d, with increasing the modulus values from 27.22 ± 5.80 g/d to 118.05 ± 6.50 g/d by ca. 294%, and 334% respectively, while the sample ID's of PET000 and PET444 are compared.

After the drawing process, as expected, the hIB fibers with a DR of 1.279 had an increased tenacity and modulus with a lower elongation, as seen in Figure 2. All samples were drawn at the same temperature of 220°C with the same DR, which is near to the maximum DRs for the treated fibers at this temperature. It was noted that the mean value of tenacity increased with an increasing of the hIB temperature, but there was no significiant difference between tenacity values at different hIB bath temperatures when standard deviation are considered for tretaed PET filaments. Interestingly, the modulus values for PET fibers produced with hIB were similar after the hot drawing for the bath temperature of 60°C, 100°C, and 125°C. The mean value for modulus relatively increased for the bath temperature of 140°C and reached 145.27 ± 9.27 g/d at the distance of 90 cm. At the production distance of 90 cm between the spin pack and the hIB tank, the difference in tenacity between the hIB and control fibers is 4.41, 4.54, 5.31, and 5.56 g/d for 60°C, 100°C, 125°C, and 140°C, respectively, in which it is clear that the differences increased by increasing the liquid temperature. The highest improvement for the tenacity is ca. 121% from 4.67 ± 0.13 g/d to 10.30 ± 0.27 g/d for tretaed fibers at the liquid temperature of 140°C. In addition, the initial modulus increased by ca. 25%, 36%, 28%, and 48% from 98.17 ± 9.46 g/d to 123.09 ± 5.60,

Table III. Fibril Diameters for Control and hIB Treated Fibers

	Fibril diameters (nm)		
	Undrawn	Drawn	
	Coarse	Coarse	Fine
PET0 (Control)	–	418.39 ± 88.27	–
PET1 (60°C)	–	215.15 ± 75.80	45.10 ± 17.10
PET2 (100°C)	–	181.94 ± 44.17	36.84 ± 11.34
PET3 (125°C)	344.44 ± 56.34	210.37 ± 39.28	37.65 ± 8.18
PET4 (140°C)	341.18 ± 83.78	196.08 ± 57.41	33.93 ± 10.78

133.64 ± 4.40, 125.61 ± 7.99, and 145.27 ± 9.27 g/d for the same hIB temperature range, respectively. The elongation percentage has similar values and remains essentially constant for the different process conditions, which are approximately between 11% and 13%.

On the contrary, an increase in tenacity became more prominent at the distance of 120 and 150 cm for the drawn control and treated fibers (see Figure 2). In addition, many fibers' breaks occurred during the drawing process for the control sample at 220°C because the control fibers were not stable at high temperature, hence easily degraded and finally broke. After many trials, a few samples were obtained, and these fibers have unusual and very low elongation at break percentage, which was about 19.28% with tenacity value of 2.06 g/d for 150 °C production distance.

It lends credence to the statement that the hIB technology has the potential to produce high tenacity and high modulus filaments at a low DR (1.279 DR), even if a low IV PET (0.65 dL/g) polymer was used. In addition, the comparison of performance analysis for the low (0.65 dL/g) and high (0.90 and 0.97 dL/g) molecular weight PET fibers spun with hIB method show no any significant difference for the undrawn and drawn fibers. Therefore, it can be concluded that the hIB method is more beneficial for the low molecular weight PET polymers. The fine structural development for the low molecular weight fibers is provided in the next sections.

Scanning Electron Microscopic (SEM) Analysis

As demonstrated in the previous studies and our work, the banded morphology is one of the most crucial parameters for hIB polyester fibers. It represents a precursor for crystallization

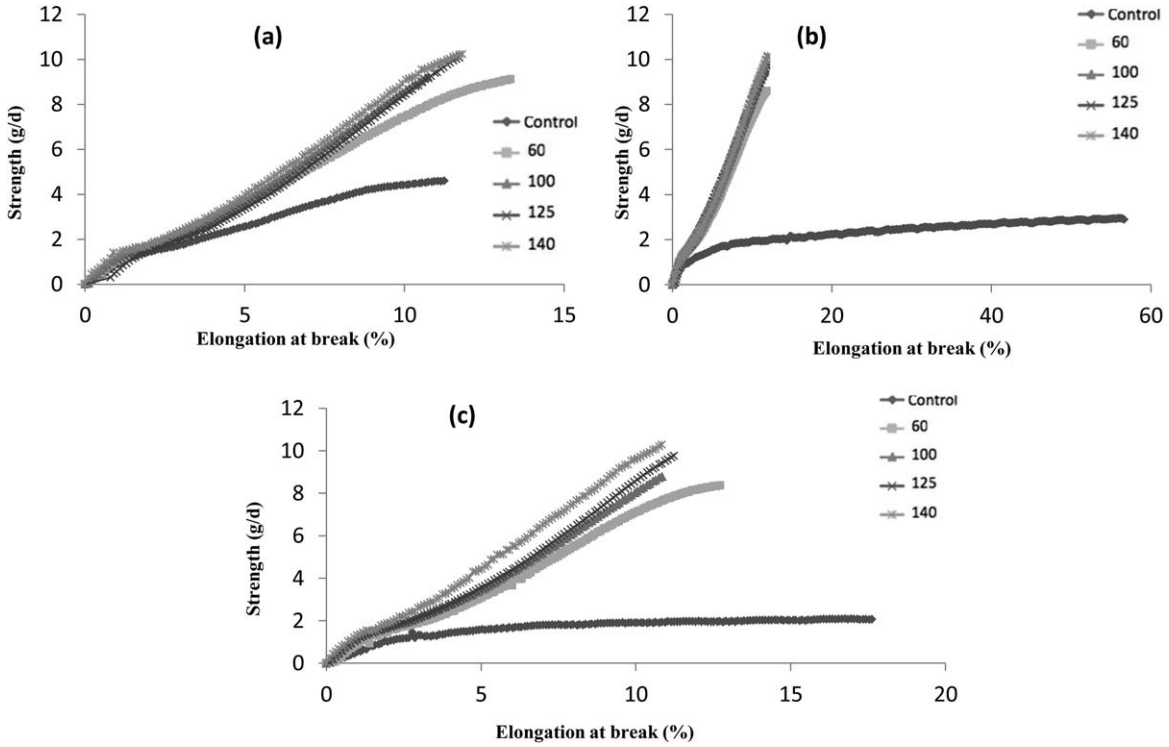

Figure 2. Comparison of the strength of drawn fibers at 1.279 DR with the drawing temperature of 220°C at (a) 90 cm, (b) 120 cm, and (c) 150 cm production distance.

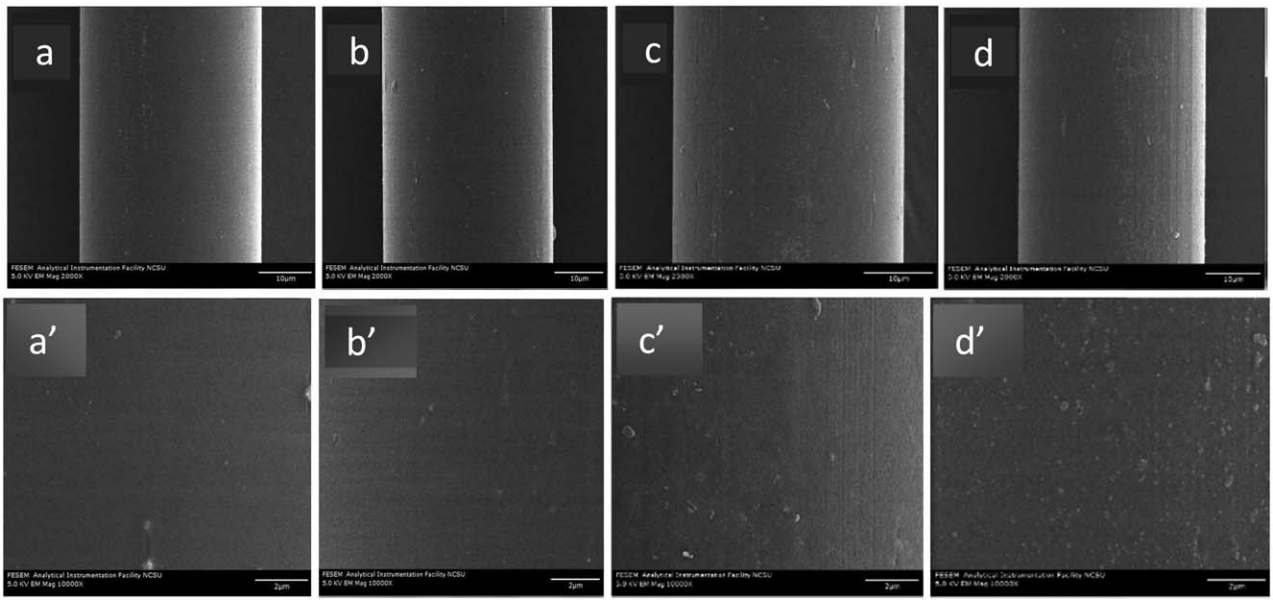

Figure 3. Low and high (letter with apostrophe) magnification of SEM images for PET as-spun fibers treated with hIB at (a) 60°C, (b) 100°C, (c) 125°C, and (d) 140°C liquid temperatures. (Scale bar = 10 and 2 μm for low and high magnifications, respectively.)

that has highly oriented amorphous structures.[7] High molecular weight PET (0.97 dL/g) filaments were spun with hIB, and then drawn at 132°C with 1.279 DR. The resulted fibers showed the banded structure for drawn and also for undrawn fibers, as seen in Figure 5. The ordering process is one of the most dominant factors to form the banded structure.[7,23] Hence, lower molecular weight PET (0.65 dL/g) fibers were analyzed based on this point. The fibers were marked in three zones to observe any possible structural changes during the drawing process. A section outside the heating tube was unheated; the second zone was the transit zone between the outside and inside drawn zone, and the third zone was the drawn zone in the tube in which the filaments was fully heated and drawn. All control and treated fibers were drawn at 1.279 DR with the drawing temperature of 220°C.

Firstly, there is no any significant difference for hIB and control fibers for surface analysis before and after the drawing process.

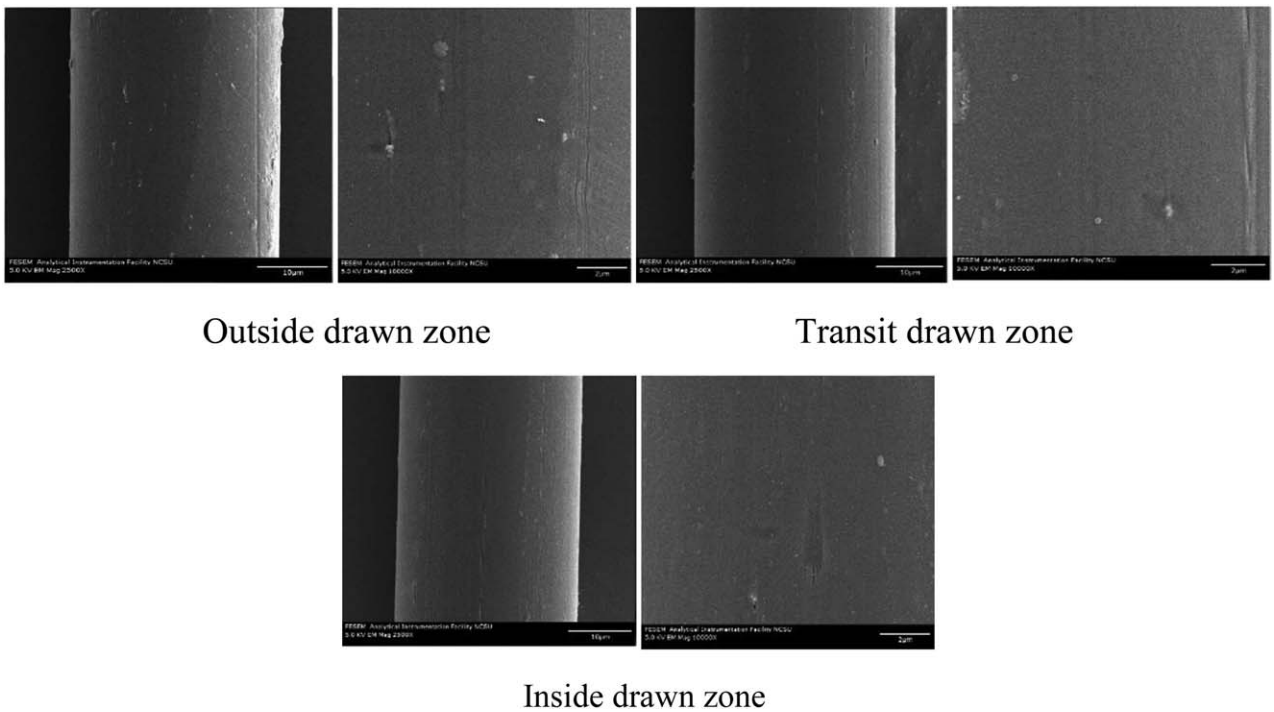

Figure 4. SEM images of drawn PET fibers spun with hIB at the temperature of 125°C. (Scale bar = 10 and 2 μm for low and high magnifications, respectively).

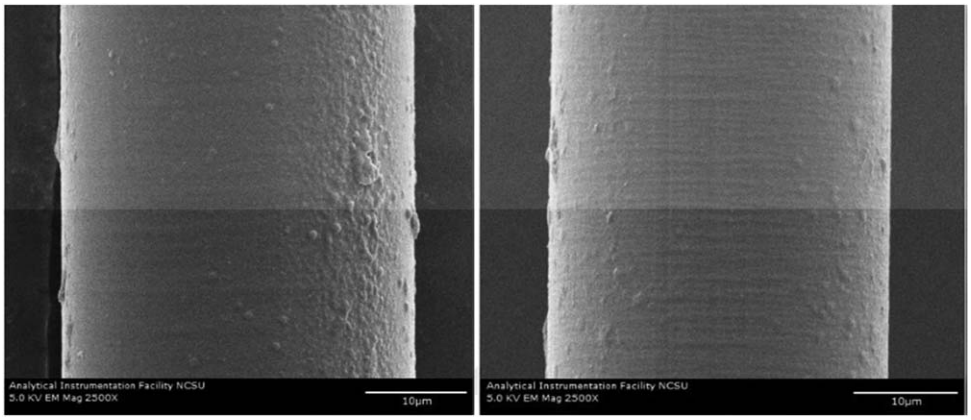

Figure 5. SEM images of PET (0.97 dL/g) fibers spun with hIB for undrawn (left) and outside drawn zone (right) fibers. (Scale bar = 10 μm).

As Figures 3 and 4 show, interestingly, there is not any banded structure either perpendicular or along the fiber axis on the hIB fiber surface for low molecular weight PET (0.65 dL/g) fibers; however, the banded structure was observed for high molecular weight fibers produced from 0.97 dL/g (Figure 5). Even if the low molecular weight fibers demonstrated superior mechanical performance for both as-spun and drawn fibers, the banded morphology was unexpectedly not observed. The formation of the banded structure can be related to the skin and core structure[24] when the skin layer has higher molecular orientation and birefringence. The molecular orientation difference between skin and core structure also should be more than a certain value. In addition, the banded morphology contains highly oriented, amorphous, crystalline, or just newly developed, less ordered crystallites with some highly entangled polymer chains.[15,25] These conclusions are coming from the structural observation of copolyester type materials.[24,25] Furthermore, the banded structure was also observed for LIB-treated polyester fibers in which the fibers also showed the smaller crystal size.[15] Firstly, the effects of the process conditions on low and high molecular weight PET might be different. Therefore, more studies with different process conditions should be done to document the development of the banded structure. However, in our case, we observed higher crystal sizes after low molecular weight (LMW) PET filaments with hIB than HMW (high molecular weight) PET fibers produced by LIB method in the past. Secondly, the difference of molecular orientation for skin-core structure might be less than a certain value which leads to the banded structure. Thirdly, the low molecular weight PET may cause less "highly entangled polymer chains" to form when compared to the high molecular weight PET. A combination of these reason(s) might possibly account for the absence of the banded morphology for the low molecular weight PET fibers spun with hIB before and after the drawing processes.

To further investigate, the fiber samples were broken in the liquid nitrogen, and the cross-section was observed via a field-emission scanning electron microscope to study the inner morphology. Figure 6 shows the fractured surface of the undrawn treated fibers. There is significant effect of the temperature of the hIB spinning system on the formation of fibrillar structures. Fibrillar structure did not form for fibers spun with hIB at the temperature of 60°C and 100°C, although they showed ultrahigh performance. This result further supports the hindrance of crystal growth under high levels of stress and appropriate temperatures in which lamellar slip can lead to *c*-axis orientation until obtaining a fully oriented structure.[26] On the other hand, fibrillar structures have been observed in fibers spun with hIB spinning systems at the temperature of 125°C and 140°C for as-spun fibers. This is very interesting and showed the dependence of crystallinity on the liquid temperature. In this experiment, it can be speculated that the mechanism for the formation of the fibrillar morphology was formed after fully oriented structure was reached and an additional extension caused a new type of deformation mechanism, which is called crystal cleavage.[26] Hence, the fibers show separation of lamellae in blocks and become more oriented to evolve into a fibrillar structure at the liquid temperature of 125°C and 140°C. X-ray data for undrawn fibers clearly supported this relationship between the fibrillar structure and the liquid temperature, which will be given in the next section. A higher hIB temperature probably increased the chains mobility to form three-dimensional arrangements of the crystals to evolve into the fibrillar structure. These fibers performed an outstanding performance with a higher degree of crystallinity and crystal size.

Figure 6 demonstrates the fractured surface of the drawn PET fibers. It is clear that the drawn and transparent fiber had a smooth surface with stretched fibrils inside in which the diameter is decreasing from the sheath to the core of the fibers. This is a strong evidence to demonstrate a highly crystallized fibrillar structure. The as-spun hIB fibers had highly ordered structures, which can be transformed into fibrillar crystals via a little hot drawing to produce high-performance filaments; this could potentially increase the fraction of taut tie molecules in amorphous regions and lead to the formation of higher orientation after the drawing processes. It has been generally accepted that polymers normally undergo chain-folding during crystallization, and microfibrils which consist of alternating chain-folded lamellae and amorphous regions to make the conventional fibers.[27] Stacked lamellae are the main reason to form the fibrils, and they are typically about 10 nm in diameter with approximately 50 nm lengths along the fiber axis.[28]

It can be seen in Figure 6 that the cross-section of the drawn PET control without hIB fiber has poorly developed, sparse

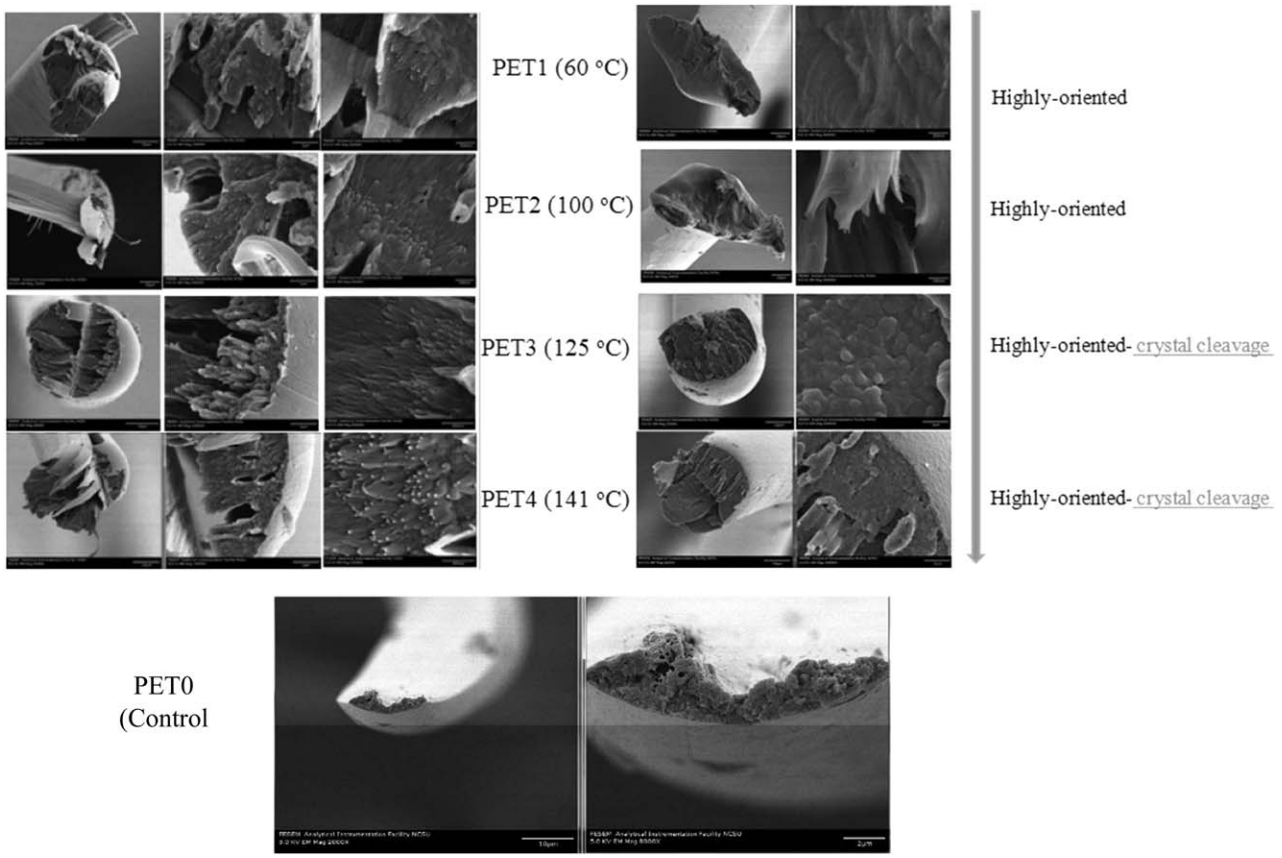

Figure 6. SEM images of cross section of undrawn (right) and drawn (left) PET fibers spun with hIB spinning system at different liquid temperatures. (For Undrawn: Scale bar = 10 and 2 μm for low and high magnifications for 60°C, 100°C, and 140°C, respectively. Scale bar = 1 μm for high magnifications for 125°C; For Drawn: Scale bar range between 10 μm and 500 nm for low and high magnifications, respectively).

fibrillar morphology after drawing at 1.279 DR with the drawing temperature of 220°C. This phenomenon is related to the fact that the traditional process produces the fibers with low strength and relatively poor occurrence of fibrillar structure. This is a weak point and is undesirable in industrial end-use applications for high performance fibers.

The further investigations of the fibril diameters are shown in Table III for control and treated fibers before and after the drawing processes. As stated previously, some poorly developed fibrils were observed for drawn control fibers with the mean diameters of more than 400 nm, but there was not any fibril for undrawn control filaments. The fibers were produced at the liquid temperature of 125°C and 140°C and had the similar fibril diameters for undrawn fibers, in which the diameters are about 350 nm. However, after the drawing process, the mean value of fibrils for PET4 is smaller than PET3. There are two distinct populations of microfibrils which are "coarse" fibril at about ~200 nm, and "fine" fibril at about ~38 nm in diameters for drawn fibers. The fibers which have been produced at the liquid temperature of 100°C, 125°C, and 140°C showed the similar "coarse" and "fine" fibrils diameters, but the 60°C liquid temperature one has a little higher mean value for the diameters, as demonstrated in Table III.

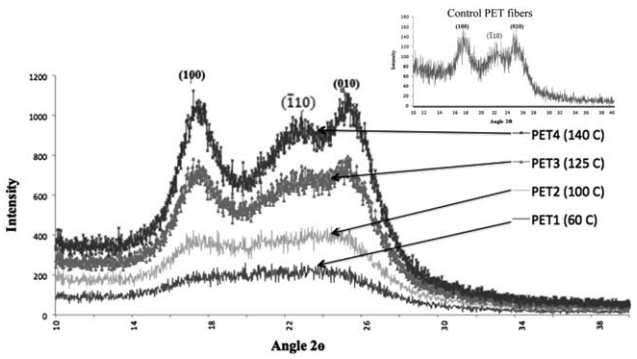

Figure 7. Equatorial X-ray diffraction profiles of PET as-spun fibers spun with hIB spinning system.

It might be speculated that we were able to demonstrate just a group of lamellae for the "fine" fibrils, which were obtained by hIB method. As Murthy *et al.*[28] have stated, the typical lamellae diameter is about 10 nm.

Wide-Angle X-ray Data Analysis

Figures 7 and 8 show the wide-angle X-ray diffraction (WAXD) patterns of the PET filaments spun without hIB and with hIB at different liquid temperatures with the distance of 90 cm. The equatorial diffraction profile was fitted using PDXL with ICDD PDF file software program. Murthy and Correale[29] have shown

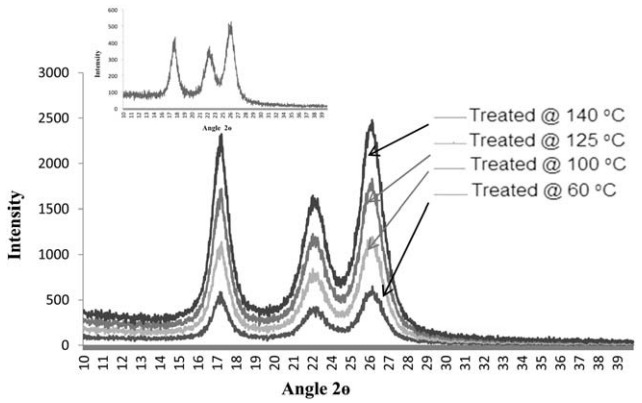

Figure 8. Equatorial X-ray diffraction profiles of drawn PET fibers spun without hIB (small figure) and with hIB.

at least two amorphous peaks, which are 17.5° and 23.5°, observed for the most "amorphous" sample.

In Figure 7, as expected, a noisy, weak diffraction of X-ray pattern was collected for undrawn control samples. However, as seen in Figure 7, using hIB method even at different process conditions demonstrated a great influence on as-spun fiber morphology. It can be seen in Figure 7 that, until the bath temperature is 125°C, the first indication is a less developed crystallites phase, which contains highly oriented PET molecules, as supported by demonstrating high tensile performance and the birefringence analysis. The filaments were produced at 60°C and 100°C, the equatorial X-ray diffraction trace is given for the hIB as-spun fibers, which only gave rise to broad, unresolved traces with high intensity which are not related to the crystals. One of the most important results of this study is that this structural phenomenon was exactly observed by SEM cross-sectional images; as we have described, there was not any fibril formation at these temperatures. In addition, the degree of crystallinity increased from 7.66% to 37.41% when the temperature of hIB increased from 60°C to 140°C (Table IV).

It is clear that increasing hIB temperature contributes to crystallization that is observed at 125°C and higher hIB temperatures. The higher hIB temperature would presumably increase the rate of crystallization, as seen in Figure 7. Low crystallinity, low elongation, and high tenacity and modulus for hIB fibers might be looked upon as the first evidence that the mostly noncrystalline chains of the hIB as-spun fibers with poorly developed crystalline are highly ordered or oriented. In addition, the amorphous phase can be divided in two-component systems, the oriented (anisotropic) and the unoriented (isotropic) components.[30] Different weak peaks in the amorphous phase can be explained as the order of different crystallographic directions and/or evidence for incipient crystalline order in samples.[29] Table IV demonstrates the crystal growth of these fibers was significantly suppressed, hence smaller apparent crystal sizes range from 13 Å to 27 Å at the hIB temperature of 60°C and 100°C when they were formed. The percent crystallinity for the control and treated fibers at the liquid temperature of 100°C is comparable; hence, it can be concluded that the treated one has a higher number of crystals because of smaller crystal sizes as demonstrated in Table IV. The highest crystallinity and crystal size were observed at 140°C liquid temperature. These prominent features of the as-spun treated filaments at the temperature of 140°C promoted crystal growth, possibly because of the increasing of local molecular mobility. Furthermore, the sharp peaks in the Figure 7 might have occurred due to the undrawn polycrystalline precursor.

After the hot drawing at 1.279 DR at the temperature of 220°C, the treated and untreated fibers show distinct crystal peaks, as observed in Figure 8. The treated fibers have gained the fibrillar structures; hence, well-developed crystals were detected at a low DR. The crystallinity and crystallite sizes were calculated by using WAXD data and are shown in Table IV. After the drawing process, the equatorial diffraction scan demonstrated better resolved peaks, indicating a more highly developed crystalline structure in which the crystal growth was significant. However, the data for untreated fibers are still noisy and weak, which points out that less developed and unoriented parts are more dominant in the morphology.

Table IV demonstrates the degree of crystallinity and crystalline dimensions for the drawn fibers. After the drawing, the apparent crystal sizes and degree of crystallinity of fibers increased for both hIB and without hIB fibers. In general, degree of crystallinity and crystallite sizes of fibers spun using hIB are greater than those of fibers without hIB treatment. After the drawing process, the degree of crystallinity has increased approximately 14% from 39.56% to 45.06% when the liquid temperature was set to 140°C. However, when the liquid temperature increased from 60°C to 140°C, the degree of crystallinity increased from 39.78% to 45.06% by ca. 13%. Despite the fact that the crystallinity for control and the fibers, which were obtained at the liquid temperature of 60°C, are close to each other, the tenacity and modulus value differences are about 94% and 25%, respectively, higher for the treated one. The occurrence of this difference is considered to be at least partly due to the fact that the

Table IV. Degree of Crystallinity and Crystalline Dimensions of PET As-Spun and Drawn (Brackets) Fibers Under Various hIB Temperatures

		Crystallite size (Å)		
hIB Temperature (°C)	Crystallinity (%)	L_{100}	$L_{\bar{1}10}$	L_{010}
-	28.92 (39.56)	29 (73)	25 (51)	36 (57)
60	7.66 (39.78)	13 (83)	17 (58)	13 (62)
100	26.51 (44.23)	23 (82)	20 (56)	27 (59)
125	32.37 (44.32)	31 (83)	25 (60)	33 (58)
140	37.41 (45.06)	40 (85)	28 (59)	34 (59)

Table V. Thermal Properties of PET As-Spun and Drawn (Brackets) Fibers Spun With and Without hIB[a]

Sample ID	Onset melting point (°C)	Peak melting point (°C)	ΔH_f^0 (J/g)	Crystallinity (%)
PET0	248.31 (249.37)	253.16 (254.05)	39.950 (52.210)	28.54 (37.29)
PET1	250.11 (249.74)	253.29 (253.75)	47.105 (55.930)	33.65 (39.95)
PET2	251.39 (252.46)	253.86 (257.88)	49.457 (61.172)	35.33 (43.69)
PET3	251.08 (256.76)	255.10 (261.38)	50.523 (59.727)	36.09 (42.66)
PET4	250.95 (256.35)	254.86 (262.56)	51.359 (63.178)	36.69 (45.13)

[a]The data was provided from the first heating curve.

result of the hot liquid that presumably caused the formation of higher crystal size, higher orientation, and the higher number of taut-tie molecules. Fibers spun with hIB at 60°C and without hIB have almost the same crystallinity level as that of the small crystal sizes for the control fibers, implying that the number of crystals is higher than that of hIB-treated fibers. Furthermore, the degree of crystallinity and crystallite size of fibers spun with hIB at the temperature of 100°C, 125°C, and 140°C has essentially the similar value as seen in Table IV.

Differential Scanning Calorimetry Data Analysis

It has been found that DSC curves do not show the state of a direct reflection of the material at room temperature.[31] During the heating process, crystallites, which are formed at low temperatures, undergo a continuous perfection process, hence partial melting and recrystallization can occur during the scan before the polymer is totally melted, which leads to an increase in the overall crystallinity.

Table V and Figure 9 present the thermal properties and DSC curves of as-spun control and its respective hIB-treated fibers made at a spinning speed of about 3000 m/min. T_g was not observed for both fibers probably because of the presence of a relatively rigid amorphous phase.[15] However, it might be observed for fibers spun at a lower take-up speed and heating rate for DSC analysis, and also for fibers with a lower degree of crystallinity. Moreover, the dual melting peak can be observed for the fibers. The first melting peak represents less developed and less ordered crystals. More ordered with greater perfection crystals for the higher temperature peak is observed with extended chain segments.

On the other hand, it can be seen that the as-spun control and treated fibers have a broad melting range from initial melting to final melting, as shown in Figure 9, which indicates a typical semi-crystalline polymer.

Table V also shows the thermal properties of PET as-spun fibers with and without using the hIB spinning system. Note that no significant increase for melting points was observed when compared with treated and control fibers, which are between 253°C and 255°C. However, the percent crystallinity has increased from 28.54% to 36.69% by ca. 29% using hIB technology at the liquid temperature of 140°C. It is beneficial in developing extended macromolecular chains to gain improvement in fiber performance. In addition, the percent of crystallinity increased from 33.65% to 36.69% by increasing the liquid temperature from 60°C to 140°C for the treated fibers.

The most prominent feature of the drawn treated fiber is the increased degree of crystallinity and melting points, as shown in Figure 9. The narrow melting peaks with lower melting points represent a low degree of crystallinity and small crystallite size present in the filaments,[18] which was also confirmed by our X-ray analysis. After the drawing process with 1.279 DR at 220°C, the treated fibers demonstrated higher temperature peaks and crystallinity. These results clearly support the transformation from a highly oriented amorphous phase to the formation of highly developed crystallites that lead to a larger portion of extended chain segments. Figure 9 shows the fibers which were produced at the liquid temperature of 140°C for as-spun and drawn samples. The highest fiber performance was observed at this temperature; therefore, the effect of production distance on fibers at the same temperature was investigated. As observed, PET fibers at the production distance of 90 cm showed the highest crystallinity and melting temperature.

Table V demonstrates that the fibers can be classified into two groups according to their onset melting temperature. The first group includes the control; the fibers were produced at 60°C and 100°C liquid temperatures with about 250°C onset temperature. The second group consists of 125°C and 140°C liquid temperatures for fibers with approximately the onset temperature of 256°C. Interestingly, these two families of fibers were exactly observed for undrawn SEM and X-ray data analysis. Peak melting temperatures increased by increasing the liquid temperature at the same production distance of 90 cm, although control and PET1 (the liquid temperature of 60°C) showed the similar temperature of about 254°C. The highest peak melting temperature was observed for 262.56°C at the liquid temperature of 140°C after just drawing with 1.279 DR at 220°C. It can be noted that the onset and melting temperature increased from 249.37°C to 256.35°C and from 254.05°C to 262.56°C by increasing of 6.98°C and 8.51°C, respectively, when control and the hIB-treated fibers were compared. This illustrates that both control and treated fibers have a different recrystallization rate during the DSC scan. The percent of crystallinity increased from 37.29% to 45.13% by ca. 21% using hIB technology at 140°C. In addition, the different liquid temperatures strongly influenced the percentage of crystallinity in which the percent of crystallinity increased from 39.95% to 45.13% by increasing the liquid temperature from 60°C to 140°C.

As stated previously, increasing the production distance between the spinneret and tank caused a decrease in the onset and peak melting points and the percent crystallinity at the same liquid

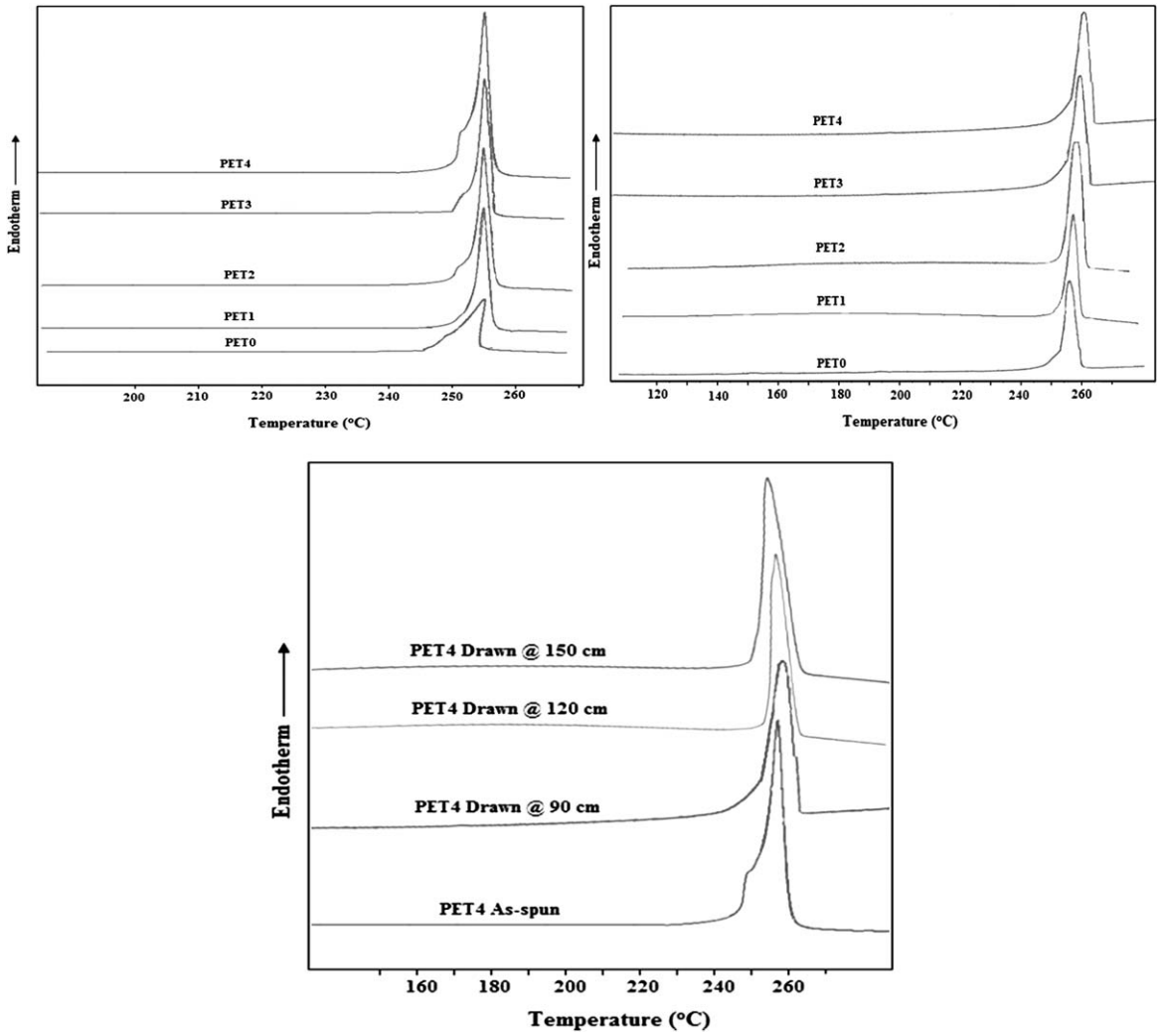

Figure 9. DSC curves of undrawn (up-left), drawn (up-right) PET fibers spun with and without hIB under different liquid temperatures, and PET4 as-spun and drawn fibers (bottom) spun with hIB at 140°C at different production distance.

temperature, as demonstrated in Table VI for the treated fibers. There is a 4.35°C and 5.04°C difference between the onset and peak melting points when the production distance increased from 90 to 150 cm, respectively. In addition, the percentage of crystallinity decreased by ca. 8.4% from 45.13% to 41.65% by increasing the production distances.

Birefringence and Density Data Analysis

The degree of molecular orientation and the extent of crystallization are two important parameters for polymer morphology, which has a strong relationship with its fiber application areas. WAXD patterns of undrawn and drawn hIB treated and untreated samples, shown in Figures 7 and 8 demonstrate significantly different crystalline structure and orientation, as shown by the intensity and sharpness of the equatorial reflections. The determination of birefringence and the indication of overall orientation is another pathway that can be employed to predict the orientation of these fibers. It is also known that the orientation has an impact on fiber modulus performance. In general, the overall orientation is affected by crystalline and the amorphous orientation factor, and the crystalline orientation factor is usually high for semi-crystalline polymeric fibers. In this case, the amorphous orientation factor is a key factor for overall orientation. In the industry, different levels of orientation can be obtained, which depends on the operating speeds.[32] If the speed is between 500 to 1500 m/min, it will yield low oriented, whereas partially oriented yarn can be produced at the speed range of 2500 and 4000 m/min. The roller and/or winder speed should be more than 6000 m/min to manufacture fully oriented materials. As mentioned before, the degree of alignment of chains along the fiber axis has a significant relation with the operation speed.

Figure 10 shows the birefringence of treated and untreated fibers at the production distance of 90 cm at about 3000 m/min take-up speed. At first glance, there is no any significant difference for the birefringence value between treated fibers at different liquid temperatures, although an increasing trend was observed with the increasing liquid temperatures. The birefringence increased from 0.195 to 0.215 and from 0.200 to 0.235 for treated as-spun and drawn fibers, respectively, by increasing the liquid temperature from 60°C to 140°C. The highest

Table VI. Thermal Properties of As-Spun and Drawn PET Fibers Spun With hIB at 140°C[a]

Sample ID	Onset melting point (°C)	Peak melting point (°C)	ΔH_f^0 (J/g)	Crystallinity (%)
PET4	250.95	254.86	51.359	36.69
PET4 drawn @ 90 cm	256.35	262.56	63.178	45.13
PET4 drawn @ 120 cm	253.53	259.37	60.627	43.31
PET4 drawn @ 150 cm	252.00	257.52	58.312	41.65

[a]The data was provided from the first heating curve.

birefringence were observed for the fibers produced at the liquid temperature of 140°C for as-spun and drawn fibers (1.279 DR) at a value of 0.215 and 0.235, respectively. The lowest birefringence was always observed for the control samples for both undrawn and drawn filaments at the value of 0.110 and 0.120, respectively. Birefringence values for as-spun and drawn control fibers are in the range as expected for the traditional melt spinning production method. At the 90 cm of production distance, the birefringence for the treated fibers with 140°C almost doubled that of the control samples for undrawn and drawn fibers. This indicates the molecular orientation level for the treated fiber is probably coming close to the highest level, as demonstrated by cross-section SEM images and X-ray data. Moreover, the effect of hot liquid with its drag force allowed us to obtain improved molecular chain orientation for lower molecular weight PET fibers during the treatment. Therefore, this highly oriented precursor hindered a poorly developed structure, which was rapidly formed during the traditional melt spinning process.

Amorphous region in the semi-crystalline polymers is divided into two main groups, namely anisotropic (oriented) and isotropic (unoriented) phases.[30] Hence, the orientation factor is strongly related with orientation degree of anisotropic phase and, in general, isotropic phase does not contribute to the overall birefringence and orientation factor. As seen in Figure 11, there is a strong correlation between the tenacity and birefringence values for undrawn and drawn fibers. The correlation for undrawn fibers of $R^2 = 0.9703$ is an exponential trend line as shown in the eq. (5).

$$y = 2.067e^{6.3434x} \quad (5)$$

where y is the tenacity (g/d) and x is the birefringence.

In addition, the correlation for drawn fibers of $R^2 = 0.9998$ is a well fit for polynomial trend line in the eq. (6).

$$y = -180.51x^2 + 112.56x - 6.2384 \quad (6)$$

where y is the tenacity (g/d) and x is the birefringence.

Figure 11 also demonstrates increased birefringence from 0.110 to 0.215 for undrawn fibers that correlates with improvement of tenacity from 4.19 to 7.97 g/d by ca. 96 and 90%, respectively. Even if the highest mean tenacity for undrawn fibers was observed at the value of 8.19 g/d with the bath temperature of 100°C, when the standard deviation is considered, tenacity for fibers that were produced at 100°C and 140°C are almost the same. Another interesting point from Figure 11 is that the undrawn fibers produced at 100°C and higher bath temperature till 140°C demonstrated almost the same performance in the terms of tenacity values and had the similar birefringence of around 0.2. Although the fibers were produced at the bath temperature of 60°C and showed the birefringence value of 0.195, these fibers demonstrated relatively lower tenacity than that of other treated as-spun fibers. It strongly indicates the birefringence value of 0.2 is an important threshold to obtain ultra-high performance PET fibers. It is also supported by the similar tenacity values for all drawn treated fibers which showed birefringence greater than 0.2 (as seen in Figure 11). The highest jump was observed for the tenacity values from undrawn to drawn fibers by ca. 38%, which were produced at the bath temperature of 60°C. This is due to the fact that the drawn fibers were obtained at this bath temperature shows the birefringence of 0.2.

It can be concluded that the bath temperature should be at least 100°C to obtain birefringence values higher than 0.2 to obtain

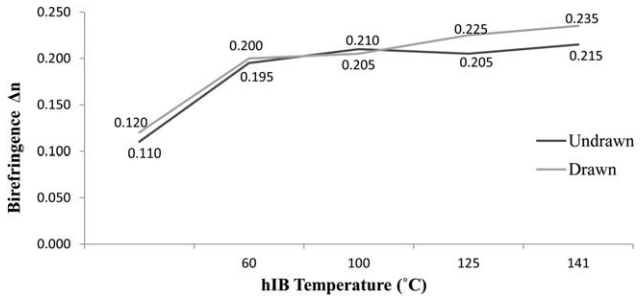

Figure 10. The relation between birefringence of treated and untreated PET fibers at various hIB temperatures for undrawn and drawn fibers.

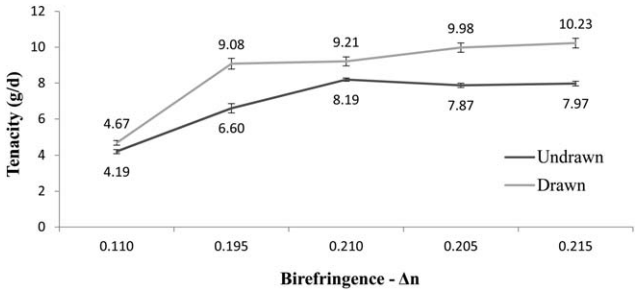

Figure 11. The relation between birefringence and tenacity of treated and untreated PET fibers at various hIB temperatures for undrawn and drawn fibers (draw ratio = 1.279) (Exponential (undrawn) $R^2 = 0.9703$, and Polynomial (drawn) $R^2 = 0.9998$).

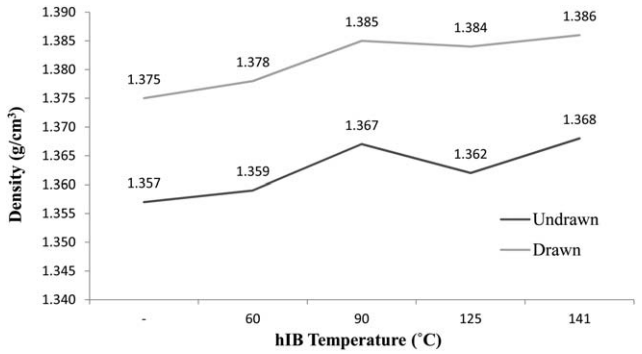

Figure 12. Fibers density of untreated and treated fibers by hIB before and after drawing process (draw ratio = 1.279).

ultra-high tenacity for the as-spun fibers. Figure 11 indicates that after the drawing process with only 1.279 DR, the fiber tenacity increased from 4.67 to 10.23 by increasing birefringence from 0.120 to 0.235 by ca. 119% and 96%, respectively. Increasing bath temperature from 60°C to 140°C caused tenacity values to improve from 9.08 to 10.23 g/d. In this case, birefringence varied from 0.200 to 0.235 by ca. 13% and 18%, respectively.

Another curious phenomenon is that the overall orientation (birefringence) has a strong influence on the fiber tenacity. The orientation is sometimes more important than the crystals' growth and crystallinity for semicrystalline polymers until a certain value of crystallinity. For example, even if the treated fibers showed the close tenacity values to each other, which were manufactured at the liquid temperature of 100°C, 125°C, and 140°C, the only fibers, which have some crystalline morphology, were observed at the bath temperature of 125°C and 140°C when Figure 7 is checked.

Figure 12 demonstrates the fibers density before and after the drawing process as a function of hIB liquid temperature at the same production distance of 90 cm and similar take-up speed of around 3000 m/min. Even if the trend for the density values was improved for as-spun fibers as the liquid temperature increased, it is hard to make a correlation between the density values and the liquid temperature. On the other hand, an exponential trend line was well fitted between the fibers' density and hIB liquid temperature for drawn fibers of $R^2 = 0.9138$. The eq. (7) for this correlation is shown below:

Table VII. Volume Fraction Crystallinity of Untreated and \ Fibers by hIB Before and After Drawing Process (draw ratio = 1.279)

Sample ID	Volume fraction crystallinity (%) for undrawn fibers	Volume fraction crystallinity (%) for drawn fiber
PET0	18.33	33.33
PET1	20.00	35.83
PET2	26.67	41.67
PET3	22.50	40.83
PET4	27.50	42.50

$$y = 1.3747e^{6E-05x} \quad (7)$$

where y is the fiber density (g/cm^3) and x is the liquid temperature (°C).

As seen in Figure 12, the as-spun fibers density increased from 1.357 to 1.368 g/cm^3 when the fibers were spun with hIB at 140°C. As the liquid temperature increased from 60°C to 140°C, the density raised from 1.359 to 1.368 g/cm^3. It is quite clear that monotonical increase in density over the range investigated for drawn fibers is an exponential trend line. The density of 1.385 g/cm^3 for the hIB spun drawn fibers at the liquid temperature of 100°C, 125°C, and 140°C was not changed significantly with the increasing liquid temperature. After drawing process, the lowest density was observed for the control sample at the value of 1.375 g/cm^3. However, the highest density value of 1.386 g/cm^3 has been demonstrated as the liquid temperature increased further to 140°C.

It is known that if a fiber has a lower crystallinity after production with a traditional high speed spinning method, usually this fiber can be more extended than that of a fiber with a higher crystallinity. As demonstrated in Table VII, the volume fraction crystallinity for untreated control sample (PET0) is lower than that of all treated fibers before and after drawing process. Thus, as expected, control fibers were able to be drawn to higher draw ratios than that of all treated fibers.

Demonstrating a low extensibility, higher birefringence, higher tenacity, and modulus show that all hIB fibers most probably have taut–tie noncrystalline chains and highly ordered amorphous phase structures. On the other hand, when the degree of crystallinity, which was obtained by X-ray (Table IV) and determined by density measurement (Table VII), was compared, the volume fraction crystallinity for as-spun PET1 (the liquid temperature of 60°C) changed drastically and became higher than that of the values for PET0 (control) fibers. These differences at least suggest that there is less formation of a void structure and higher orientation of chains for treated fibers, which were formed during the hIB processes. A reason for the formation of void structure is generally associated with the use of much higher take-up speeds for the melt spinning methods. In Table VII, the volume fraction crystallinity increased from 18.33% to 27.50% when the fibers were treated at the liquid temperature of 140°C by ca. 50% for as-spun fibers. For the drawn fibers, the crystallinity improved by ca. 28% from 33.33% to 42.50% at a DR of 1.279 with the drawing temperature of 220°C when the fibers spun with hIB at the temperature of 140°C. The effect of the liquid temperature on the volume fraction crystallinity for treated fibers is also significant and increased from 20.00% to 27.50% and from 35.83 to 42.50 by increasing the liquid temperature from 60 to 140°C for as-spun and drawn fibers, respectively. Despite the fact that the crystallinity for drawn PET2, PET3, and PET4 are close to each other, it cannot be stated that these fibers should have also similar crystallinity before the drawing process (see Table VII).

CONCLUSIONS

Ultra-high strength as-spun and drawn PET fibers with unique properties were produced by using a horizontal isothermal bath

(hIB). This study is the first known report of a production of high-strength PET filament from a lower molecular weight polymer having IV of 0.65 dL/g. The highest tenacity was observed more than 8 and 10 g/d for as-spun and drawn fibers, respectively.

At the liquid temperature of 60°C and 100°C and the production distance of 90 cm, the fibers demonstrated relatively higher tenacity and modulus values than that of the distance of 120 and 150 cm. However, when the liquid temperatures were fixed to 125°C and 140°C, the tenacity and modulus values came close to each other at three different production distances for undrawn fibers. The effects of production distances became a more prominent feature for the drawn fibers for their mean modulus performance at different liquid temperatures. Increasing production distance caused a decrease in the modulus of fibers for each liquid temperature. Therefore, almost all other characterization methods for the fibers which were presented in this study were obtained from the production distance of 90 cm.

SEM analysis indicates that there was not any banded structure either perpendicular or along the fiber axis on the hIB treated fiber surface for PET fibers. In addition, the significant effect of the temperature of the hIB spinning system on fibrillar structure was demonstrated. The fibrillar structure has not been observed for fibers spun with hIB at the temperature of 60°C and 100°C, although the fibrillar structures was formed at the liquid temperature of 125°C and 140°C for the as-spun fibers. The fibrillar morphology can be formed after a fully oriented structure was reached but, interestingly, we probably obtained this unique structure for undrawn fibers at the liquid temperature of 125°C and 140°C with the liquid depth and production distance of 20 and 90 cm, respectively. Strong similarities were found when SEM images of cross-section and X-ray diffraction for the as-spun treated fibers were compared. If the equatorial X-ray diffraction profile showed clear crystalline peaks that caused us to observe the fibrillar structure in the cross-section for the same fiber.

Other characterization methods in this work, such as DSC, X-ray, birefringence, etc., demonstrated that the resulted as-spun fibers developed a rare formation of precursors for crystallization with a highly oriented structure which transformed into a highly crystallized fibrillar structure after only drawing at 1.279 DR at the drawing temperature of 220°C.

Depending on the process conditions for the PET fibers, the precursor for the crystallization can be formed during the drawing process at the drawing temperature higher or closer to its T_g at a very high DR and strain rate. However, the precursor can be developed, as we observed during the hIB melt spinning process where certain conditions are satisfied. As clearly demonstrated by cross-section of SEM images and X-ray data for the undrawn treated fibers, the type of precursor can be different according to the liquid temperatures. The effects of a higher level threadline tension and the lower liquid temperatures, while cooling at a very slow rate, restricted for the fibers the formation and growth of crystallites; however, this probably increased the residual frozen-in orientation and the higher rate of motion of neighboring chain segments, which promoted the occurrence of tree-dimensional structure when fibers were treated at higher liquid temperatures. This phenomenon may also lead to a higher molecular orientation. Furthermore, at a higher liquid temperature, the threadline temperature is much higher than the T_g of the polymer. Hence, there is a greater probability to form three-dimensional arrangements and obtain more developed crystals for the as-spun fibers (Figure 7).

Finally, this study contributes a further understanding of the structure development of lower molecular weight PET fibers spun via hIB with highly improved mechanical and thermal properties.

REFERENCES

1. Wang, L. A.; Wang, Y. W.; Deng, Z. X.; Xia, X. L.; Liu, W. T.; Han, S. Q.; Zhu, C. S. *Adv. Mat. Res.* **2011**, *332–334*, 526.
2. Wu, G.; Zhou, Q.; Chen, J. Y.; Hotter, J. F.; Tucker, P. A.; Cuculo, J. A. *J. Appl. Polym. Sci.* **1995**, *55*, 1275.
3. Hobbs, T.; Lesser, A. *J. Polymer* **2000**, *41*, 6223.
4. Wu, G.; Jiang, J. D.; Tucker, P. A.; Cuculo, J. A. *J. Polym. Sci. Part B: Polym. Phys.* **1996**, *34*(12), 2035.
5. Ito, M.; Takahashi, K.; Kanamoto, T. *J. Appl. Polym. Sci.* **1990**, *40*, 1257.
6. Wu, G.; Cuculo, J. A. *J. Appl. Polym. Sci.* **1995**, *56*, 869.
7. Chen, P.; Afshari, M.; Cuculo, J. A.; Kotek, R. *Macromolecules* **2009**, *42*, 5437.
8. Nicholson, T. M.; Davies, G. R.; Ward, I. M. *Polymer* **1994**, *35*, 4259.
9. Carr, P. L.; Nicholson, T. M.; Ward, I. M. *Polym. Adv. Technol.* **1997**, *8*, 592.
10. Welsh, G. E.; Blundell, D. J.; Windle, A. H. *J. Mater. Sci.* **2000**, *35*, 5225.
11. Zaroulis, J. S. Temperature, Strain Rate and Strain State Dependence of Evaluation of Mechanical Behavior and Structure of Poly(ethylene terephthalate) with Finite Strain Deformation. MS Thesis, Massachusetts Institute of Technology, Cambridge, MA, March, **1996**.
12. Alfonso, G. C.; Verdona, M. R.; Wasiak, A. *Polymer* **1978**, *19*, 711.
13. Smith, F.; Steward, R. *Polymer* **1974**, *15*, 283.
14. Lu, X. F; Hay, J. N. *Polymer* **2001**, *42*(19), 8055.
15. Hotter, J. F.; Cuculo, J. A.; Tucker, P. A.; Annis, B. K. *J. Appl. Polym. Sci.* **1998**, *69*, 2051.
16. Cuculo, J. A. (NC State University). U.S. Patent US005149480A, September 22, **1992**.
17. Cuculo, J. A. (NC State University). U.S. Patent US005733653A, March 31, **1998**.
18. Lin, C. Y.; Tucker, P. A.; Cuculo, J. A. *J. Appl. Polym. Sci.* **1992**, *46*, 531.
19. Wang, I. C.; Dobb, M. G.; Tomka, J. G. *J. Text. Inst.* **1995**, *86*, 383.
20. Avci, H. Novel Approaches to the Development and Characterization of Antimicrobial Conventional and Nanostructured

Materials. MS thesis, North Carolina State University: Raleigh, NC, March **2010**.

21. Duhovic, M.; Bhattacharyya, D.; Fakirov, S. *Macromol. Mater. Eng.* **2010**, *295*, 95.
22. Chen, J. Y.; Tucker, P. A.; Cuculo, J. A. *J. Appl. Polym. Sci.* **1997**, *66*, 2441.
23. Abou-Kandil, A. I.; Windle, A. H. *Polymer* **2007**, *48*, 4824.
24. Takeuchi, Y.; Shuto, Y.; Yamamoto, F. *Polymer* **1988**, *29*(4), 605.
25. Abou-Kandil, A.; Windle, A. H. *Polymer* **2007**, *48*, 4824.
26. Ohta, T. *Polym. Eng. Sci.* **1983**, *23*(13), 697.
27. Mukhopadhyay, S.; Deopura, B. L.; Alagirusamy, R. *J. Ind. Text.* **2004**, *33*(4), 245.
28. Murthy, N. S.; Grubb, D. T. *J. Polym. Sci. Part B: Polym. Phys.* **2003**, *41*, 1538.
29. Murthy, N. S.; Correale, S. T.; Minor, H. *Macromolecules* **1991**, *24*, 1185.
30. Harget, P. J.; Oswald, H. J. *J. Polym. Sci. Polym. Phys. Ed.* **1979**, *17*(3), 531.
31. Holdsworth, P. J.; Turner-Jones, A. *Polymer* **1971**, *12*, 195.
32. Karacan, I. *Fibers Polym.* **2005**, *6*(3), 186.